

# The Gas-Phase Absorption Spectrum of a Neutral GFP Model Chromophore

L. Lammich,\* M. Åxman Petersen,<sup>†</sup> M. Brøndsted Nielsen,<sup>†</sup> and L. H. Andersen\*

\*Department of Physics and Astronomy, University of Aarhus, Aarhus, Denmark; and <sup>†</sup>Department of Chemistry, University of Copenhagen, Copenhagen, Denmark

**ABSTRACT** We have studied the gas-phase absorption properties of the green fluorescent protein (GFP) chromophore in its neutral (protonated) charge state in a heavy-ion storage ring. To accomplish this we synthesized a new molecular chromophore with a charged NH<sub>3</sub> group attached to a neutral model chromophore of GFP. The gas-phase absorption cross section of this chromophore molecule as a function of the wavelength is compared to the well-known absorption profile of GFP. The chromophore has a maximum absorption at 415 ± 5 nm. When corrected for the presence of the charged group attached to the GFP model chromophore, the unperturbed neutral chromophore is predicted to have an absorption maximum at 399 nm in vacuum. This is very close to the corresponding absorption peak of the protein at 397 nm. Together with previous data obtained with an anionic GFP model chromophore, the present data show that the absorption of GFP is primarily determined by intrinsic chromophore properties. In other words, there is strong experimental evidence that, in terms of absorption, the conditions in the hydrophobic interior of this protein are very close to those in vacuum.

## INTRODUCTION

Many colors appearing in nature stem from absorption of visible light by chromophore molecules in photoactive proteins. The green color of leaves, for example, is due to strong chromophore absorption in the blue and red parts of the spectrum. Different colors may reflect intrinsic properties of the various chromophores as well as complicated tunings that shift the electronic energy levels within the proteins hosting the chromophores. Organisms use photoactive proteins with a variety of different chromophores to sense and harvest light in their environment. The eye makes use of one particular chromophore, retinal, and color vision is based on molecular interactions with this particular chromophore in the *trans*-membrane vision proteins. It is worth mentioning that George Wald was awarded the Nobel Prize in 1967 for his important work on the molecular basis for color vision (1), but it took almost 40 years before gas-phase experiments established the sign of the changes in the absorption (i.e., blue/red shift) that vision proteins exert on the chromophore (2). This emphasizes very well the importance of local molecular interactions but also the difficulty of describing the influence of biological environments at the molecular level.

In this work we focus on the question to what extent molecular properties in the gas-phase, i.e., properties of completely isolated chromophore molecules, are relevant to biological systems. Our strategy is to monitor interactions by observing shifts in the absorption profile of chromophore molecules in different hosting environments like vacuum, solutions, and photoactive proteins. The absorption profile, typically in the visible part of the spectrum, reflects the

electronic energy levels and hence carries direct information on such perturbations. Organic chromophores having large conjugated electronic systems are indeed sensitive to external charges and dipoles as well as hydrogen bonding and steric constraints. Hence they are convenient reporters on local environments in, e.g., proteins.

Because of its fluorescent properties and numerous applications in molecular and cell biology, the green fluorescent protein (GFP) is a particularly well-studied and important photoactive protein (3). It consists of 238 amino acids in a single chain folded into a so-called  $\beta$ -barrel. At the center of the  $\beta$ -barrel sits the fluorescent chromophore. It forms part of the protein chain and originates from an autocatalytic cyclization and subsequent oxidation of three amino-acid residues of the protein: serine (Ser)-65, tyrosine (Tyr)-66, and glycine (Gly)-67. The chromophore, which is well protected from the bulk solvent, consists of a phenolic and an imidazolidinone ring (see Fig. 1) rigidly held within the  $\beta$ -barrel, forming a fluorescent  $\pi$ - $\pi^*$  electron system (3–5). The surrounding cavity contains a number of charged residues in the vicinity of the chromophore and four water molecules that are important in establishing a hydrogen-bonding network around it (6).

A number of gas-phase measurements of chromophore anions and cations of the GFP family have been reported recently (7–13). These studies together with studies of the photoactive yellow protein (14) strongly indicate that in terms of absorption, these proteins provide a very gentle host environment, close to a vacuum.

It seems evident, however, that the interaction between the chromophore and the protein is indeed important for some of the special properties of GFP. For example, the chromophore only fluoresces in the presence of the protein (15), which is probably related to the hindrance of *cis-trans* isomerization in the excited state (16) because of space constraints in the

Submitted July 20, 2006, and accepted for publication September 19, 2006.

Address reprint requests to M. Brøndsted Nielsen, E-mail: mbn@kiku.dk; or L. H. Andersen, E-mail: lha@phys.au.dk.

© 2007 by the Biophysical Society

0006-3495/07/01/201/07 \$2.00

doi: 10.1529/biophysj.106.093674

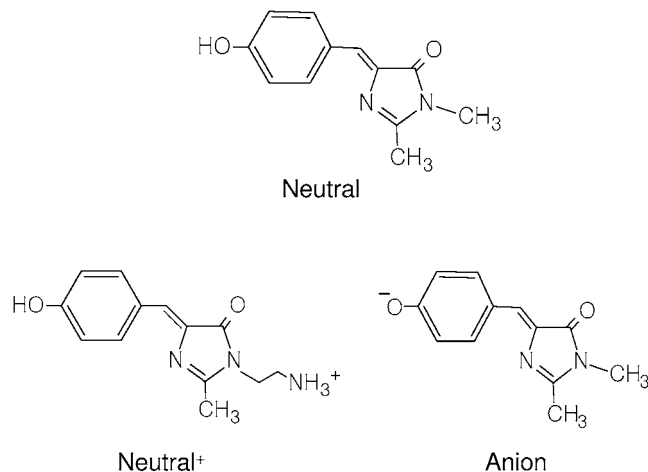


FIGURE 1 Model chromophores of GFP: The “Neutral” model chromophore (top), the neutral chromophore with a positively charged side group “Neutral<sup>+</sup>” synthesized in this study (left), and the deprotonated “Anion” model chromophore used in the previous work (7) (right).

rigid protein (17). Moreover, the large shift of the emission into the green part of the spectrum upon near-UV absorption is caused by a proton-transfer reaction to a nearby amino-acid group with the chromophore in the first excited singlet state (18).

At the same time, the fluorescence emission of GFP exhibits no time dependence (17). This is surprising, since the electronic transition might be associated with significant changes in the chromophore dipole moment, and one might expect a hosting medium to relax in response to the changes in electrostatic interaction. Such time-dependent fluorescence shifts have been observed in other protein environments (19,20). The absence of a measurable shift in fluorescence for GFP may be due to a lack of sensitivity of the protein medium to the chromophore dipole moment (i.e., the chromophore-protein interaction being too weak). Alternatively, the protein might be so rigid that little or no relaxation occurs on the timescale of the excited-state lifetime (17).

To estimate the effect of a specific perturbation on, for example, the position of the absorption maximum one may study proteins with mutations near the chromophore. Alternatively, one can make use of advanced theory (see, e.g., (16,21–26)). However, such calculations must be compared to measurements to establish their reliability, and for this purpose, absorption data recorded under vacuum conditions are necessary.

The absorption spectrum of the green fluorescent protein is special in the sense that it exhibits two maxima, one at 479 nm, which is ascribed to the excitation of a deprotonated (anion) chromophore, and a main peak at 397 nm, which supposedly correlates to a protonated (neutral) chromophore (3). For the first time, we here address experimentally the absorption of an isolated *neutral* GFP model chromophore. To this end we have synthesized a novel molecule, which carries a positive charge well separated from a neutral

chromophore, which is akin to that in GFP. Indeed, by studying two chromophores of GFP with different protonation stages we will have much firmer ground when it comes to conclusions about the degree of vacuumlike conditions that possibly may exist inside the protein cavity.

## EXPERIMENTAL

### Chromophore models

The storage-ring technique is only applicable to ions and therefore a new model chromophore was designed to mimic the true neutral GFP chromophore. The salt  $\text{H}^+\text{Cl}^-$  was prepared in three steps starting from 4-(4-acetoxybenzylidene)-2-methyl-4H-oxazol-5-one (27) and ethylenediamine. The detailed synthesis will be published elsewhere. The new chromophore is essentially a neutral chromophore with a charged group attached to it. The model chromophore is shown in Fig. 1 together with the previously used deprotonated (anion) model chromophore and a true neutral model chromophore.

### Solution spectra

Absorption spectra of model chromophores in solutions are recorded by a UV/Vis spectrophotometer (ThermoSpectronic Helios- $\alpha$ , Bie & Berntsen, Rødovre, Denmark).

### Gas phase spectra

To measure the absorption spectra of the model chromophores, gas-phase ions are stored in an ion storage ring, ELectrostatic Ion Storage ring Aarhus (ELISA), (28,29) shown in Fig. 2. We irradiate the ions with a laser pulse of tunable wavelength, and ions that absorb a photon increase their internal energy, and hence, temperature, accordingly (for a discussion of the temperature of small systems and the statistical decay of hot ions see Andersen et al. (13,30)). Due to the increased energy, the ions eventually break apart creating fragments, some of which are neutral. By recording the yield of neutral fragments as a function of the wavelength we obtain the relative absorption cross section as explained below.

The gas-phase ions are produced in an electrospray ion source (31). The neutral GFP model chromophore (Neutral<sup>+</sup>, Fig. 1) is dissolved in methanol. The solution is pumped through a fused silica capillary to a stainless-steel needle with a bias voltage of  $\sim 3$  kV. From the needle, the solution is electrosprayed toward the entrance of the ion source. In the ion source the charged droplets are transported through a heated capillary where the solvent is evaporated, and thus the chromophore ions go into the gas phase. The ions are then accumulated in a 22-pole cylindrical ion trap (32). In the trap, helium is used as a buffer gas to cool the ions. After 100-ms accumulation time the ions are extracted as a bunch containing  $\sim 10^4$  ions. The ions are then accelerated to 22 kV

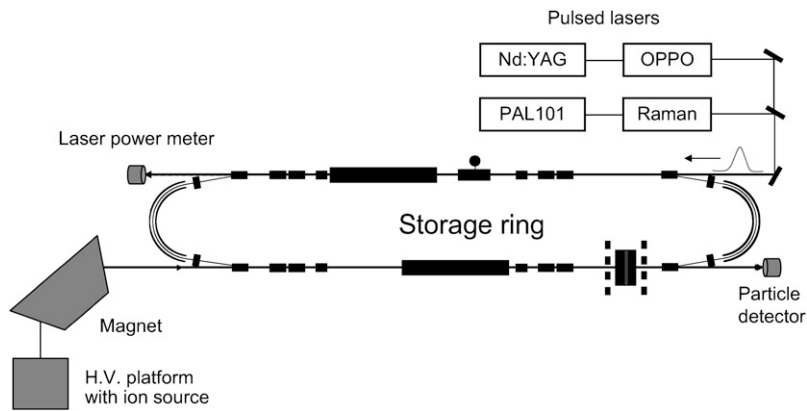


FIGURE 2 The electrostatic ion storage ring ELISA equipped with an electrospray ion source, pulsed lasers, and a detector for neutral products.

and mass-to-charge selected (mass 246 amu) by a bending magnet. Finally, the ions are injected into the storage ring, where they circulate with a revolution time of 63  $\mu\text{s}$  and a lifetime of a few seconds.

At the end of one of the straight sections of ELISA, a microchannel plate detector is positioned (see Fig. 2). If ions in this section fragment by means of a collision or by photon absorption (see below), neutral fragments are formed that continue on straight trajectories into the detector. Counts from the detector are accumulated as a function of the time after injection, so the time evolution of the neutral fragment production can be followed (see Fig. 3).

The ions are stored for 45 ms in ELISA before they are exposed to the laser pulse. At this time the background count rate is almost constant and solely due to collisions with residual gas in the ring (pressure  $\sim 10^{-11}$  mbar). A tunable nanosecond laser pulse is fired along the straight section opposite the injection side at a repetition rate of 10 Hz corresponding to one laser shot at each ion bunch injected into ELISA (see

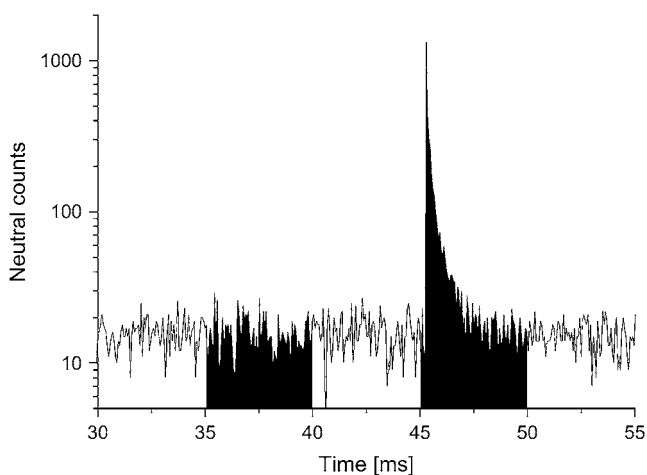


FIGURE 3 Counts of neutral fragments from the Neutral<sup>+</sup> GFP model chromophore as a function of time after injection into ELISA. Note that the laser induces a signal which is here two orders-of-magnitude above the background count rate ( $\lambda = 397$  nm,  $E_{\text{pulse}} = 0.55$  mJ).

Fig. 2). The laser is synchronized with the injection of ions into ELISA and the timing is adjusted to ensure maximum overlap with the ion bunch. Photoabsorption will result in a breakup of the ions, thus creating neutral fragments, which are detected if the dissociation takes place in the injection section. The fragmentation happens over an appreciable time (ms) and the storage technique is thus essential for detecting the delayed (statistical) action of the excitation.

To cover the desired wavelength range we use a pulsed alexandrite laser (PAL101, Light Age, Somerset, NJ) in combination with a Raman cell. The alexandrite laser is tunable in the range 720–800 nm. The second harmonic is then either used directly, or sent into a Raman cell. This provides wavelengths in the regions 360–399 nm (second harmonic) and 412–430 nm (first Stokes in  $D_2$ ). In the region from 424 nm to 450 nm, we used an Optical Parametric Power Oscillator (OPPO, Lambda Physik, Göttingen, Germany) pumped by the third harmonic of an Nd:YAG laser (Infinity, Coherent, Santa Clara, CA). After interaction with the ion bunch the laser pulse leaves the ring, and the pulse energy is measured with a power meter. The laser-pulse energy is averaged over the data-acquisition time, which is 200 s corresponding to 2000 injections at each wavelength  $\lambda$ .

### Data analysis

Typical data with the number of counts from the detector as a function of time for the Neutral<sup>+</sup> chromophore model are shown in Fig. 3. The laser-induced signal is clearly seen. The counts are summed from the time of laser interaction to the time, where the neutral count rate is reduced to the background level giving  $N_{\text{signal}}(\lambda)$  (second black window in Fig. 3). The average number of background counts ( $N_0$ ) is determined by summing up the counts in a time window before the laser interaction, but after a stable background rate is reached (first black window in Fig. 3). The background counts are subtracted from the counts in the signal-time window and also used as a measure of the number of ions in the storage ring, i.e., for normalization. The resulting fraction is termed the yield,  $Y(\lambda)$ :

$$Y(\lambda) = \frac{N_{\text{signal}}(\lambda) - N_0}{N_0} \quad (1)$$

The yield was found to depend approximately linearly on the photon flux for low laser-pulse energies, whereas at higher energies it saturates, as seen in Fig. 4. The typical pulse energy ( $E_{\text{pulse}}$ ) during the measurement of the absorption profile is 0.2 mJ, which is within the linear range. Thus, we further normalize the yield to the photon flux, which is proportional to  $E_{\text{pulse}} \times \lambda$ . The relative absorption cross section is then

$$\sigma_{\text{abs}}(\lambda) \propto \frac{Y(\lambda)}{E_{\text{pulse}} \times \lambda} \quad (2)$$

Here we assume that the quantum yield for photofragmentation is wavelength-independent, that the pulse energy is sufficiently low to avoid saturation, and that the spatial overlap between the ion bunch and the laser pulse remains constant during the measurement of the absorption profile. Only relative absorption cross sections are given here since the laser overlap and the total number of ions in the ring is not known on an absolute scale.

## RESULTS AND DISCUSSION

The measured absorption profiles of the gas-phase GFP chromophores (Neutral<sup>+</sup> and Anion) are shown in the lower panel of Fig. 5. The top panel shows for comparison the wild-type GFP absorption profile (33). The deprotonated (anion) absorption curve in the gas-phase is from a previous work (7). It is evident that the gas-phase data seem to confirm the earlier charge-state assignments of the chromophores inside the GFP, although the main GFP peak also matches very well that of a positively charged model chromophore

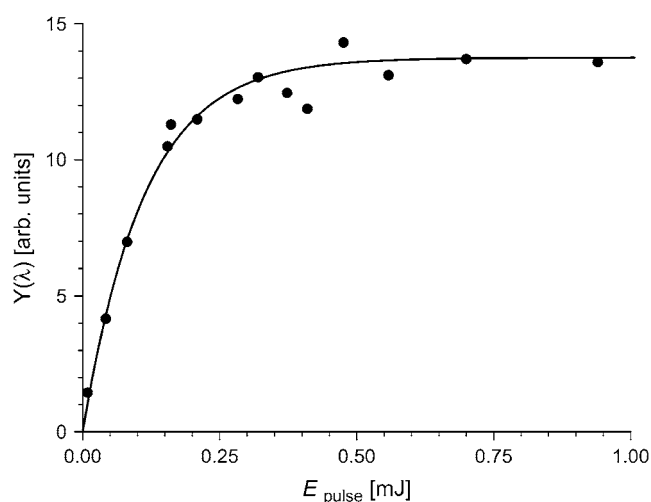


FIGURE 4 The yield of fragmentation as a function of the average laser-pulse energy for the neutral model chromophore ( $\lambda = 397$  nm). The solid line is a fit ( $Y = a(1 - \exp(-bE_{\text{pulse}}))$ ) to the data, which shows approximate linearity at low laser-pulse energy.

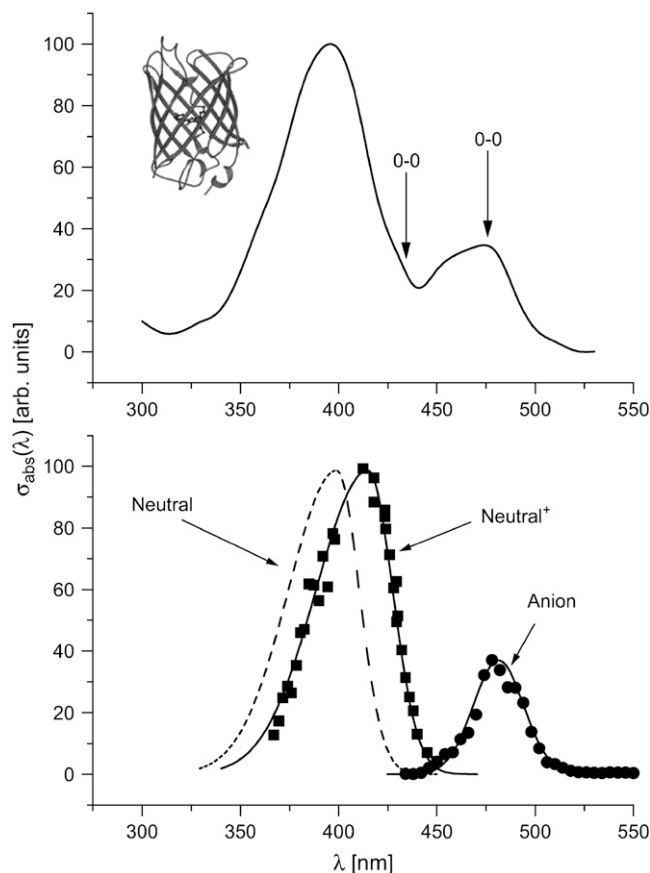


FIGURE 5 (Top) Absorption of GFP with a protonated (neutral) chromophore (large peak) and a deprotonated (anion) chromophore (small peak) (33). The 0-0 transition wavelengths obtained from hole-burning experiments (34) are indicated. (Bottom) Gas-phase absorption cross sections for the protonated (Neutral<sup>+</sup>) and the deprotonated (Anion) GFP model chromophores (see Fig. 1). Data for the anion model chromophore are taken from Nielsen et al. (7). The relative height of the two peaks recorded in the gas-phase is adjusted to approximately match the two peaks of the protein absorption curve. The dashed line corresponds to the estimated gas-phase absorption of a neutral GFP chromophore without a charged group (see text).

(9). It is noted that the peak widths in the protein and in the gas-phase are rather similar and probably mainly determined by the Franck-Condon overlap to various vibrational states in the first electronically excited state  $S_1$ .

Unfortunately, our present laser systems cannot provide light between 399 and 412 nm, which is close to the absorption maximum in the protein (397 nm). Moreover, since we used different laser systems with potentially different beam overlaps, the left- and right-hand sides of the absorption peak for the Neutral<sup>+</sup> chromophore are not a priori calibrated with respect to each other in terms of the strength of the absorption signal. Thus we used a fitting procedure with two “half” Gaussian functions with different heights and widths but the same (fitted) wavelength for the absorption maximum. After the fit the two sets of data were scaled relative to each other to yield the same cross section at the absorption maximum, which is found to be at  $415 \pm 5$  nm.

To estimate the inherent perturbation from the positive  $\text{NH}_3$  group in the present  $\text{Neutral}^+$  model chromophore we performed Gaussian03 TDDFT calculations at the B3LYP/6-311++G\*/MP3 level of theory (35). The  $S_0$ - $S_1$  transition of the true neutral model chromophore (terminated by two methyl groups in the imidazolino ring) was found at 359 nm, whereas the transition wavelength of the  $\text{Neutral}^+$  model chromophore with a charged group and one methyl group (see Fig. 1) was calculated to be at 372 nm. According to this, the presence of the positive charge causes a red shift of 13 nm equivalent to an energy shift of 0.12 eV (an energy shift of 0.16 eV was calculated with a B3LYP/6-31G(d) optimized structure). If we correct the measured peak position of the  $\text{Neutral}^+$  model chromophore (415 nm) for this energy shift, we obtain a transition wavelength of 399 nm for the neutral GFP chromophore in vacuum, which is indeed very close to the main absorption peak of GFP. We note that the calculation does not reproduce the absorption maximum of the gas-phase measurement very well (415 vs. 372 nm), yet we assume that the obtained energy shift produced by the presence of the charged group is more reliable than the absolute energy levels.

The geometry optimized structure of the  $\text{Neutral}^+$  chromophore is shown in Fig. 6. It reveals that the  $\text{Neutral}^+$  chromophore adopts a conformation where the lactam oxygen forms a hydrogen bond to one of the ammonium hydrogens with an  $\text{O}\cdots\text{H}$  distance of 1.7 Å (MP3 optimized) and 1.4 Å (B3LYP/6-31+G(d) optimized). We are currently targeting neutral GFP chromophores where the ionic spectator group is not able to form hydrogen bonds.

To see the effect of a solvent, we recorded the spectrum of the  $\text{Neutral}^+$  chromophore in methanol. The solvent caused a significant 45-nm blue shift, as seen in Fig. 7. A sizeable blue shift was also observed for the anionic chromophore in solutions (7–9). The absorption of another neutral model chromophore of GFP was studied in solutions theoretically and experimentally by Voityuk et al. (36) and by Niwa et al. (15). Different solvents gave here an absorption maximum in the interval between 368 nm and 376 nm, which is close to the wavelength where we observe a maximum in absorption

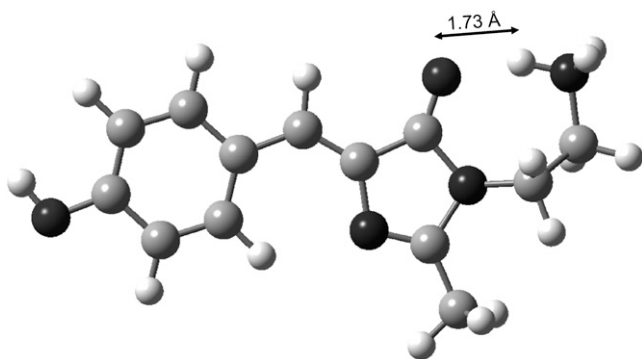


FIGURE 6 MP3 geometry optimized structure of the  $\text{Neutral}^+$  chromophore.

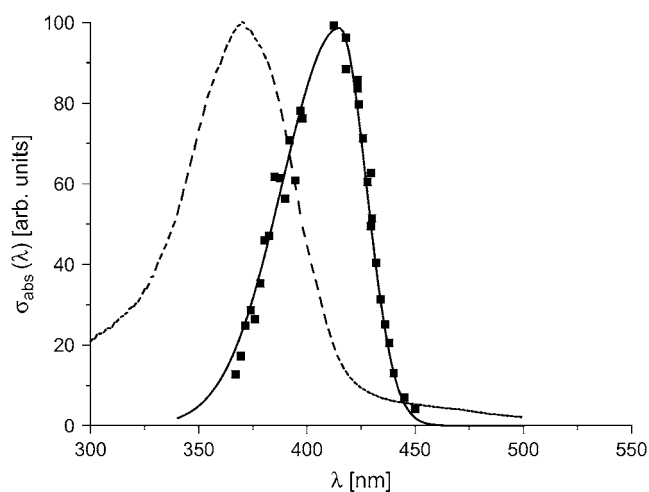


FIGURE 7 Absorption spectra of the  $\text{Neutral}^+$  model chromophore in a methanol solution (*dashed*) and in the gas-phase.

of  $\text{Neutral}^+$  in methanol (370 nm). The conclusion is clear: there are significant perturbations on the electronic levels in solutions.

It is evident that the wavelength for maximum absorption of the anionic as well as neutral chromophores in vacuum are very close to the wavelengths of the corresponding peaks in the protein (see Fig. 5 and Table 1). This is well in line with predictions that the protein environment exerts little twist on the chromophore, which is planar in the gas-phase. Calculations suggest that the two ring planes of the chromophore are displaced by  $0.9^\circ$  (dihedral angle) for the deprotonated chromophore and  $10.9^\circ$  for the neutral chromophore in the protein environment (37). It is also worth noting that the conditions in proteins are reflected in their dielectric constant. In bulk water the dielectric constant is  $\sim 80$ , whereas a value at least 10 times smaller may be used for the interior of proteins (38). This emphasizes that there may be little charge-shielding inside proteins. Naturally, this depends critically on the protein as well as the specific location in the protein; a single dielectric constant cannot represent the permittivity everywhere in an inhomogeneous and anisotropic protein environment.

The present as well as earlier experimental results (7) are in full agreement with the recent theoretical finding of Sinicropi et al. (26), who find that the protein cavity provides an environment

TABLE 1 Absorption maxima of GFP compared to absorption maxima for GFP model chromophores in vacuum

Host medium	Charge state	$T$ (K)	$\lambda_{\text{max}}$ (nm)	$\Delta E$ (eV)	Reference
GFP	0	300	396	3.13	(18)
GFP	0	77	404	3.07	(18)
Vacuum	0	$\sim 300$	$399 \pm 5$	$3.12 \pm 0.04$	This work
GFP	-1	300	476	2.61	(18)
GFP	-1	77	471	2.63	(18)
Vacuum	-1	$\sim 300$	479	2.59	(7)

for the anionic GFP chromophore where different perturbations like the presence of counterions balance each other both in the  $S_0$  and  $S_1$  states and give very little disturbance on the electronic and molecular structure of the chromophore.

We come to the conclusion that the absorption properties of the green fluorescent protein to a high degree are determined by the intrinsic chromophore properties. GFP as well as photoactive yellow protein (14) provide very good shielding of their chromophores. The neighboring amino acids in the protein cage may cause protonation or deprotonation of the chromophore, which is indeed important because it may shift the absorption significantly as shown by this work.

It is interesting to compare these findings with the situation for retinal containing photoactive proteins. In the case of rhodopsin, which contains retinal in the protonated Schiff-base form, an even bigger shift is observed upon a change in the protonation stage. The protonated retinal chromophore has a maximum absorption at 610 nm in vacuum (2) but it shifts to  $\sim 380$  nm when it becomes deprotonated (39), which happens in the rhodopsin intermediate metarhodopsin II and in UV-sensing pigments. Unlike the situation for chromophores in GFP, retinal in the protonated Schiff-base form is subject to significant perturbations from the opsin protein, which forms the basis for color vision.

## CONCLUSIONS

A new molecule with a charged  $\text{NH}_3$  group attached to a neutral model chromophore of the green fluorescent protein was studied in the gas-phase. The absorption cross section of the chromophore as a function of the wavelength is very close to the main absorption peak of the green fluorescent protein. These data, together with previous data of an anionic GFP chromophore (7), provide strong evidence for the almost vacuumlike conditions that exist for  $S_0$  and  $S_1$  at the ground-state equilibrium geometry of the chromophore in the protein. Evidently, the protein interactions mainly have a significant influence on the photoinduced dynamics in the excited state.

We thank Steen Brøndsted Nielsen for stimulating discussion on this work.

This work was supported by the Lundbeck and Velux Foundations, and the Danish Research Agency (contracts No. 21-03-0330 and No. 2111-04-0018).

## REFERENCES

1. Wald, G. 1968. Molecular basis of visual excitation. *Science*. 162: 230–239.
2. Andersen, L. H., I. B. Nielsen, M. B. Kristensen, M. O. A. E. Ghazaly, S. Haacke, M. B. Nielsen, and M. Petersen. 2005. Absorption of Schiff-base retinal chromophores *in vacuo*. *J. Am. Chem. Soc.* 127:12347–12350.
3. Tsien, R. Y. 1998. The green fluorescent protein. *Annu. Rev. Biochem.* 67:509–544.
4. Zimmer, M. 2002. Green fluorescent protein (GFP): applications, structure, and related photophysical behavior. *Chem. Rev.* 102:759–782.

5. Prendergast, F. G. 1999. Biophysics of the green fluorescent protein. *Methods Cell Biol.* 58:1–18.
6. Ormö, M., A. B. Cubitt, K. Kallio, L. A. Gross, R. Y. Tsien, and S. J. Remington. 1996. Crystal structure of the *Aequorea victoria* green fluorescent protein. *Science*. 273:1392–1395.
7. Nielsen, S. B., A. Lapierre, J. U. Andersen, U. V. Pedersen, S. Tomita, and L. H. Andersen. 2001. Absorption spectrum of the green fluorescent protein chromophore anion *in vacuo*. *Phys. Rev. Lett.* 87:228102.
8. Andersen, L. H., A. Lapierre, I. B. Nielsen, S. B. Nielsen, U. V. Pedersen, S. U. Pedersen, and S. Tomita. 2002. Photo-absorption studies of chromophores at ELISA storage ring. *Nucl. Phys. Rev.* 19:176–179.
9. Andersen, L. H., A. Lapierre, S. B. Nielsen, I. B. Nielsen, S. U. Pedersen, U. V. Pedersen, and S. Tomita. 2002. Chromophores of the green fluorescent protein studied in the gas phase. *Eur. Phys. J. D.* 20:597–600.
10. Boyé, S., S. B. Nielsen, H. Krogh, I. B. Nielsen, U. V. Pedersen, A. F. Bell, X. He, P. J. Tonge, and L. H. Andersen. 2003. Gas-phase absorption properties of DsRed model chromophores. *Phys. Chem. Chem. Phys.* 5:3021–3026.
11. Boyé, S., I. B. Nielsen, S. B. Nielsen, H. Krogh, A. Lapierre, H. B. Pedersen, S. U. Pedersen, U. V. Pedersen, and L. H. Andersen. 2003. Gas-phase absorption properties of a green fluorescent protein-mutant chromophore: the W7 clone. *J. Chem. Phys.* 119:338–345.
12. Boyé, S., H. Krogh, I. B. Nielsen, S. B. Nielsen, S. U. Pedersen, U. V. Pedersen, L. H. Andersen, A. F. Bell, X. He, and P. J. Tonge. 2003. Vibrationally resolved photoabsorption spectroscopy of red fluorescent protein chromophore anions. *Phys. Rev. Lett.* 90:118103.
13. Andersen, L. H., H. Bluhme, S. Boyé, T. J. D. Jørgensen, H. Krogh, I. B. Nielsen, S. B. Nielsen, and A. Svendsen. 2004. Experimental studies of the photophysics of gas-phase fluorescent protein chromophores. *Phys. Chem. Chem. Phys.* 6:2617–2627.
14. Nielsen, I. B., S. Boyé-Péronne, M. O. A. E. Ghazaly, M. B. Kristensen, S. B. Nielsen, and L. H. Andersen. 2005. Absorption spectra of photoactive yellow protein chromophores in vacuum. *Biophys. J.* 89:2597–2604.
15. Niwa, H., S. Inouye, T. Hirano, T. Matsuno, S. Kojima, M. Kubota, M. Ohashi, and F. I. Tsuji. 1996. Chemical nature of the light emitter of the *Aequorea* green fluorescent protein. *Proc. Natl. Acad. Sci. USA.* 93:13617–13622.
16. Toniolo, A., S. Olsen, L. Manoha, and T. Martinez. 2004. Conical intersection dynamics in solution: the chromophore of green fluorescent protein. *Faraday Discuss.* 127:149–163.
17. Jaye, A. A., D. Stoner-Ma, P. Matousek, M. Towrie, P. J. Tonge, and S. R. Meech. 2006. Time-resolved emission spectra of green fluorescent protein. *Photochem. Photobiol.* 82:373–379.
18. Brejc, K., T. Sixma, P. Kitts, S. Kain, R. Tsien, M. Ormö, and S. Remington. 1997. Structural basis for dual excitation and photoisomerization of the *Aequorea victoria* green fluorescent protein. *Proc. Natl. Acad. Sci. USA.* 94:2306–2311.
19. Ghose, M., S. Mandal, D. Roy, R. Manda, and G. Basu. 2001. Dielectric relaxation in a single tryptophan protein. *FEBS Lett.* 509: 337–340.
20. Cohen, B. E., T. B. McAnaney, E. S. Park, Y. N. Jan, S. G. Boxer, and L. Y. Jan. 2002. Probing protein electrostatics with a synthetic fluorescent amino acid. *Science*. 296:1700–1703.
21. Weber, W., V. Helms, J. A. McCammon, and P. W. Langhoff. 1999. Shedding light on the dark and weakly fluorescent states of green fluorescent proteins. *Proc. Natl. Acad. Sci. USA.* 96:6177–6182.
22. Voityuk, A. A., M.-E. Michel-Beyerle, and N. Rösch. 1998. Quantum chemical modeling of structure and absorption spectra of the chromophore in green fluorescent proteins. *Chem. Phys.* 231:13–25.
23. Helms, V. 2002. Electronic excitations of biomolecules studied by quantum chemistry. *Curr. Opin. Struct. Biol.* 12:169–175.
24. Marques, M. A. L., X. López, D. Varsano, A. Castro, and A. Rubio. 2003. Time-dependent density-functional approach for biological chromophores: the case of the green fluorescent protein. *Phys. Rev. Lett.* 90:258101.

25. Martin, M. E., F. Negri, and M. Olivucci. 2004. Origin, nature, and fate of the fluorescent state of the green fluorescent protein chromophore at the CASPT2/CASSCF resolution. *J. Am. Chem. Soc.* 126:5452–5464.
26. Sinicropi, A., T. Andruniow, N. Ferre, R. Basosi, and M. Olivucci. 2005. Properties of the emitting state of the green fluorescent protein resolved at the CASPT2/CASSCF/CHARMM level. *J. Am. Chem. Soc.* 127:11534–11535.
27. Kojima, S., H. Ohkawa, T. Hirano, S. Maki, H. Niwa, M. Ohashi, S. Inouye, and F. I. Tsuji. 1998. Fluorescent properties of model chromophores of tyrosine-66 substituted mutants of *Aequorea* green fluorescent protein (GFP). *Tetrahedron Lett.* 39:5239–5242.
28. Møller, S. P. 1997. ELISA, an electrostatic storage ring for atomic physics. *Nucl. Instrum. Meth. Phys. Res. A.* 394:281–286.
29. Andersen, L. H., O. Heber, and D. Zajfman. 2004. Physics with electrostatic rings and traps. *J. Phys. B.* 37:R57–R88.
30. Andersen, J. U., E. Bonderup, and K. Hansen. 2001. On the concept of temperature for a small isolated system. *J. Chem. Phys.* 114:6518–6525.
31. Andersen, J. U., P. Hvelplund, S. B. Nielsen, S. Tomita, H. Wahlgreen, S. P. Møller, U. V. Pedersen, J. S. Forster, and T. J. D. Jørgensen. 2002. The combination of an electrospray ion source and an electrostatic storage ring for lifetime and spectroscopy experiments on biomolecules. *Rev. Sci. Instrum.* 73:1284–1287.
32. Gerlich, D. 1993. Experimental investigations of ion-molecule reactions relevant to interstellar chemistry. *J. Chem. Soc. Faraday Trans.* 89:2199–2208.
33. Morise, H., O. Shimomura, F. H. Johnson, and J. Winant. 1974. Intermolecular energy-transfer in bioluminescent systems of *Aequorea*. *Biochemistry.* 13:2656–2662.
34. Bonsma, S., R. Purchase, S. Jezowski, J. Gallus, F. Konz, and S. Volker. 2005. Green and red fluorescent proteins: photo- and thermally induced dynamics probed by site-selective spectroscopy and hole burning. *ChemPhysChem.* 6:838–849.
35. Frisch, M. J., G. W. Trucks, H. B. Schlegel, G. E. Scuseria, M. A. Robb, J. R. Cheeseman, J. A. Montgomery, Jr., T. Vreven, K. N. Kudin, J. C. Burant, J. M. Millam, S. S. Iyengar, J. Tomasi, V. Barone, B. Mennucci, M. Cossi, G. Scalmani, N. Rega, G. A. Petersson, H. Nakatsuji, M. Hada, M. Ehara, K. Toyota, R. Fukuda, J. Hasegawa, M. Ishida, T. Nakajima, Y. Honda, O. Kitao, H. Nakai, M. Klene, X. Li, J. E. Knox, H. P. Hratchian, J. B. Cross, V. Bakken, C. Adamo, J. Jaramillo, R. Gomperts, R. E. Stratmann, O. Yazyev, A. J. Austin, R. Cammi, C. Pomelli, J. W. Ochterski, P. Y. Ayala, K. Morokuma, G. A. Voth, P. Salvador, J. J. Dannenberg, V. G. Zakrzewski, S. Dapprich, A. D. Daniels, M. C. Strain, O. Farkas, D. K. Malick, A. D. Rabuck, K. Raghavachari, J. B. Foresman, J. V. Ortiz, Q. Cui, A. G. Baboul, S. Clifford, J. Cioslowski, B. B. Stefanov, G. Liu, A. Liashenko, P. Piskorz, I. Komaromi, R. L. Martin, D. J. Fox, T. Keith, M. A. Al-Laham, C. Y. Peng, A. Nanayakkara, M. Challacombe, P. M. W. Gill, B. Johnson, W. Chen, M. W. Wong, C. Gonzalez, and J. A. Pople. 2004. Gaussian 03, Revision C.02. Gaussian, Inc., Wallingford, CT.
36. Voityuk, A. A., A. D. Kummer, M.-E. Michel-Beyerle, and N. Rösch. 2001. Absorption spectra of the GFP chromophore in solution: comparison of theoretical and experimental results. *Chem. Phys.* 269:83–91.
37. Marques, M. A. L., X. Lopez, D. Varsano, A. Castro, and A. Rubio. 2003. Time-dependent density-functional approach for biological chromophores: the case of the green fluorescent protein. *Phys. Rev. Lett.* 90:258101.
38. Havranek, J. J., and P. B. Harbury. 1999. Tanford-Kirkwood electrostatics for protein modeling. *Proc. Natl. Acad. Sci. USA.* 96:11145–11150.
39. Nielsen, I. B., M. Å. Petersen, L. Lammich, M. B. Nielsen, and L. H. Andersen. 2006. Absorption studies of neutral retinal Schiff Base chromophores. To appear in *J. Phys. Chem. A.*